PROCEEDINGS OF SCIENCE

High-mass star formation expored with maser VLBI & thermal (ALMA, JVLA) observations

Luca Moscadelli*
INAF-Osservatorio di Arcetri, Largo E. Fermi 5, Firenze (Italy)
E-mail: mosca@arcetri.astro.it

Intense methanol and water maser transitions are commonly observed towards high-mass young stellar objects (YSO). Multi-epoch very long baseline interferometry (VLBI) observations allow us to determine maser positions and three-dimensional velocities with an accuracy of about 1 mas and 1 km s^{-1}, respectively. Presently, JVLA cm and ALMA mm observations can determine the spatial distribution and (line of sight) kinematics of the thermal (continuum and line) emission around the forming star with unprecedented sensitivity ($\sim$10 μJy and $\sim$1 mJy for continuum and line, respectively) and angular resolution (0.″05-0.″2). Combining maser VLBI and thermal interferometric datasets is the most accurate way to determine the physical conditions and unveil the dynamical structures (disks, jets, expanding/infalling shells) associated with massive star formation. This talk presents the results of this technique for two massive star forming regions: G16.59−0.05 and G24.78+0.08, whose maser emission has been extensively monitored with VLBI and for which we have recently obtained new JVLA and ALMA data.

14th European VLBI Network Symposium & Users Meeting (EVN 2018)
8-11 October 2018
Granada, Spain

*Speaker.

PoS(EVN2018)005

1. Introduction

In the last decade, interferometric (particularly ALMA and JVLA) observations have clearly indicated that the formation of low-mass up to early-B type stars follows a common route, involving accretion disks and jets [2]. The formation of the more distant and faster forming O-type ($\geq 20 M_\odot$) stars is not equally well characterized by observations, and could proceed through a different path, as predicted by the "competitive accretion" model [3]. Although disks and jets around young stellar objects (YSO) have been observed, we still lack a deeper characterization of their properties. Among the still open problems, particularly relevant are 1) the role played by turbolence, and gravitation and magnetic fields in regulating the infall of the YSO's envelope, and the rotation and (possibly) fragmentation of the disk, and 2) the mechanism to launch and collimate the protostellar jet. For OB-type YSOs, it is also essential to understand how the energetic UV radiation from nuclear burning can affect the preexisting accretion/ejection structures, by ionizing and exerting strong radiation pressure on the circumstellar gas. In this regard, it is important to study the hypercompact (HC) HII regions ($\leq$0.03 pc in size and $\geq 10^{10}$ pc cm^{-6} in emission measure), which represent the first step in the ionization/expansion of an ionized region around a newly born early-type star.

In this work, we present sensitive, high-angular resolution (0.″1–0.″2) JVLA and ALMA observations of: 1) a disk+jet system around an early-B type YSO in the star-forming region G16.59−0.05, and 2) an HC HII region in the star-forming region G24.78+0.08. This latter case study, where we have also employed multi-epoch very long baseline interferometry (VLBI) observations of molecular masers to determine the three-dimensional (3D) kinematics of the circumstellar gas, provides a good example of the synergy between interferometric thermal and maser VLBI observations.

2. A disk+jet system around a $10 M_\odot$ YSO in G16.59−0.05

We employed ALMA to observe G16.59−0.05 during Cycle 3 in September 2016 [8]. The ALMA FWHM beam was $\approx$0.″15. The correlator frequency setup consisted of six spectral windows (SPW), one broad 2 GHz spectral unit to obtain a sensitive continuum measurement at $\approx$242 GHz, and five narrower SPWs to cover a large number of lines, in particular the CH_3CN (J = 14-13), $C^{34}S$ (J = 5–4), and CH_3OH rotational transitions. In G16.59−0.05, the most massive YSO is well identified by the positional correspondence of the compact JVLA 22 GHz continuum with the Subaru 24.5 μm emission [4]. In the following we will refer to this YSO as Bm. Previous sensitive JVLA A-Array observations at 6, 13, and 22 GHz have detected a radio jet emerging from Bm, elongated $\approx 3''$ along the E-W direction [4, 7]. Our recent ALMA data reveals that a well-defined SW-NE, Local Standard of Rest (LSR) velocity ($V_{\rm LSR}$) gradient is detected at the position of Bm in all the observed high-density gas tracers. Looking at Fig. 1, we note that the JVLA 22 GHz continuum, pinpointing the YSO, falls just between the SW blue-shifted and the NE red-shifted line emission, and that the direction of the $V_{\rm LSR}$ gradient forms a large ($\approx$70°) angle with the radio jet traced by the extended JVLA 13 GHz continuum. These findings suggest that the $V_{\rm LSR}$ gradient can be due to rotation of the gas in an envelope and/or disk surrounding the YSO. The P-V plot produced along the axis (at PA = 18°) of the $V_{\rm LSR}$ gradient confirms that we are observing

envelope-disk rotation. It has a butterfly-like shape, with well-defined spurs at high absolute velocities and small offsets in the second and fourth quadrants. These spurs correspond to gas whose line of sight velocity increases with decreasing radius and could be consistent with Keplerian rotation.

Since the molecular emission at high blue- ($\leq$56 km s^{-1}) and red-shifted ($\geq$63 km s^{-1}) velocities is approximatively compact, we have fitted a two-dimensional (2D) Gaussian profile and determined the peak position at each velocity channel. Figure 2 (left panel) shows that the spatial distribution of the high-velocity emission of CH_3OH is elongated at PA = 18$\pm$3°, which we take as the direction of the major axis of the molecular disk around the high-mass YSO Bm. Along the red-shifted side, $\approx$0.″15 or $\approx$500 au in extent, the gas $V_{\rm LSR}$ increases monotonically approaching the YSO, ranging from $\approx$62 km s^{-1} up to $\approx$69 km s^{-1}. On the contrary, the blue-shifted side of the disk is traced only at the lowest velocities, 50–55 km s^{-1}. Figure 2 (right panel) plots $V_{\rm LSR}$ versus positions projected along the disk major-axis, and shows the best-fit Keplerian curve. We derive a value for the YSO mass of $M_\star \sin^2(i) = 10 \pm 2\ M_\odot$, where i ($60° \leq i \leq 120°$) is the inclination of the disk rotation axis with the line of sight. Inside the disk radius of $\approx$0.″15 (or $\approx$500 au), the 1.2 mm continuum flux is 42 mJy, corresponding to $\approx$1 $M_\odot$. Since this value is much less than the YSO mass $\approx$10 $M_\odot$, our choice of fitting a Keplerian velocity profile appears to be well justified "a-posteriori".

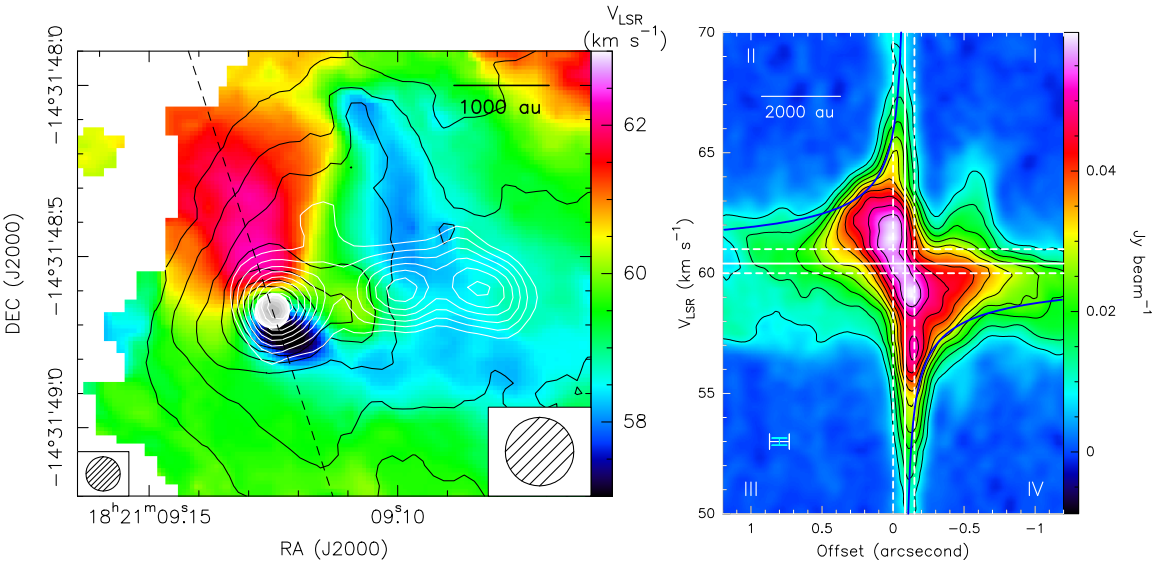

Figure 1: Gas kinematics towards the high-mass YSO Bm [8]. *Left panel:* the black contours and the color map show, respectively, the velocity-integrated intensity and the intensity-averaged velocity of the $C^{34}S$ J = 5–4 line (E_u = 28 K). The grey-scale filled and white contours show the JVLA 22 GHz and 13 GHz continuum emission, respectively. The JVLA beams at 22 and 13 GHz are reported in the bottom left and right corners, respectively. *Right panel:* P-V plot of the $C^{34}S$ J = 5–4 line. The cut (at PA = 18°) along which positions are evaluated is indicated with the dashed black line in the left panel. The horizontal and vertical white continuous lines, and the blue curves mark, respectively, the $V_{\rm LSR}$ and positional offset of the YSO, and the Keplerian profile around a YSO of 10 $M_\odot$.

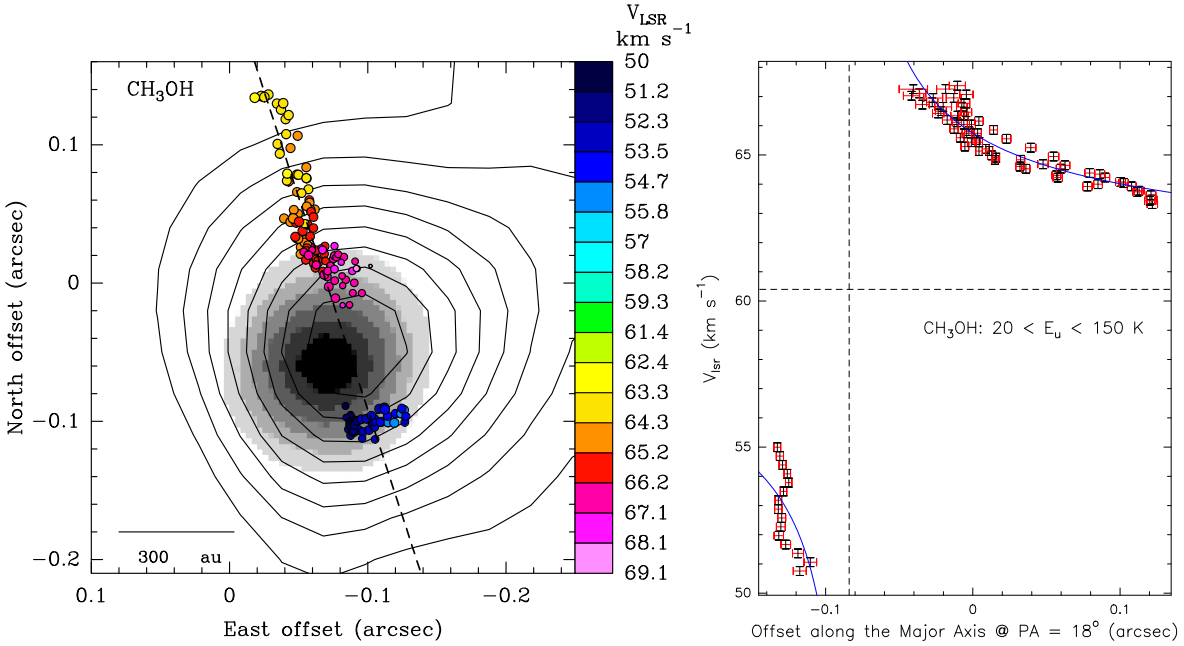

Figure 2: *Left panel:* The disk around the high-mass YSO Bm. Colored dots indicate the peak positions of the most blue- and red-shifted velocity channels for the emission of nine unblended CH_3OH lines with $20\ \mathrm{K} \leq E_u \leq 900$ K. Colors represent $V_{\rm LSR}$ as coded on the right of the panel. The dashed black line, at PA = 18°, shows the linear fit to the spatial distribution of the channel peaks. The grey-scale filled and black contours represent the JVLA 22 and 13 GHz continuum, respectively, with the same levels as in Fig. 1. *Right panel:* Black and red errorbars give, respectively, major-axis projected positions and $V_{\rm LSR}$ (together with the corresponding errors) for the highest-velocity emission peaks of six CH_3OH lines with $20\ \mathrm{K} \leq E_u \leq 150$ K. The blue curve is the best Keplerian fit to the data. The horizontal and vertical dashed lines indicate the fitted YSO $V_{\rm LSR}$ and position, respectively.

3. The HC HII region in G24.78+0.08

Inside the most prominent molecular core (named A1) of the high-mass star forming region G24.78+0.08 (bolometric luminosity of $\sim 2\times10^5\ L_\odot$ at a distance of 7.2±1.4 kpc), VLA A-Array (1.3 cm and 7 mm) observations have revealed an intense (~10 mJy beam^{-1} at 1.3 cm), hypercompact (size≈1000 au) HII region [1, 5]. Our Cycle 2 (July and September 2015), high-angular resolution (0.″2) ALMA observations has detected strong emission in the H30α line (at 231901 MHz) emerging from the HC HII region [6]. We have probed the kinematics of the ionized gas by studying how the position of the compact H30α emission changes in velocity, by fitting the emission in the channel maps with a 2D Gaussian profile. Figure 3 (right panel) reveals that a well-defined $V_{\rm LSR}$ gradient is observed in the H30α line. It is directed at PA = 39° (about parallel to the major axis of the VLA 7 mm continuum image) and extends over quite a large velocity range, from ≈85 km s^{-1} to ≈139 km s^{-1} going from SW to NE. The velocity gradient, 22 km s^{-1} mpc^{-1}, is one of the highest so far observed towards HC HII regions. The dynamical mass inferred from this $V_{\rm LSR}$ gradient is $M_{dyn} \geq 96\ M_\odot$, much larger than the mass of the late-O type ionizing star,

≈20 $M_\odot$, estimated from the radio and bolometric luminosity. That rules out the interpretation of the V_{LSR} pattern in terms of rotation/infall. The simplest interpretation of the observed V_{LSR} gradient in the H30α line is in terms of a fast, bipolar ouflow blowing from the massive YSO, placed at the center of the H30α pattern and responsible for the gas ionization. Figure 3 (left panel) reveals that a SW-NE V_{LSR} gradient (about parallel to that seen in the ionized gas) is also observed in the molecular gas surrounding the HC HII region, which indicates that the molecular and ionized gas share a similar motion.

The interaction of the fast-moving ionized gas with the surrounding molecular environment is also traced with both water and methanol masers. While water masers arise just at the border of the ionized gas, methanol masers are observed at relatively larger separation from the center of the HC HII region (see Fig. 3, right panel). Figure 4 shows the 3D velocities of the water and methanol masers, derived via multi-epoch, sensitive VLBA and EVN observations, respectively. The water maser proper motions witness the fast (≈40 km s^{-1}) expansion of dense, shocked circumstellar gas towards N and E of the HC HII region [5]. Methanol masers are observed to the N, SE and S of the HC HII region, and their overall motion indicates expansion away from the ionized gas at significantly lower velocities (mainly ≤10 km s^{-1}) than the water masers.

Future studies on this object will determine the degree of collimation of the ionized flow and test whether we are observing the onset of the stellar wind from an O-type star.

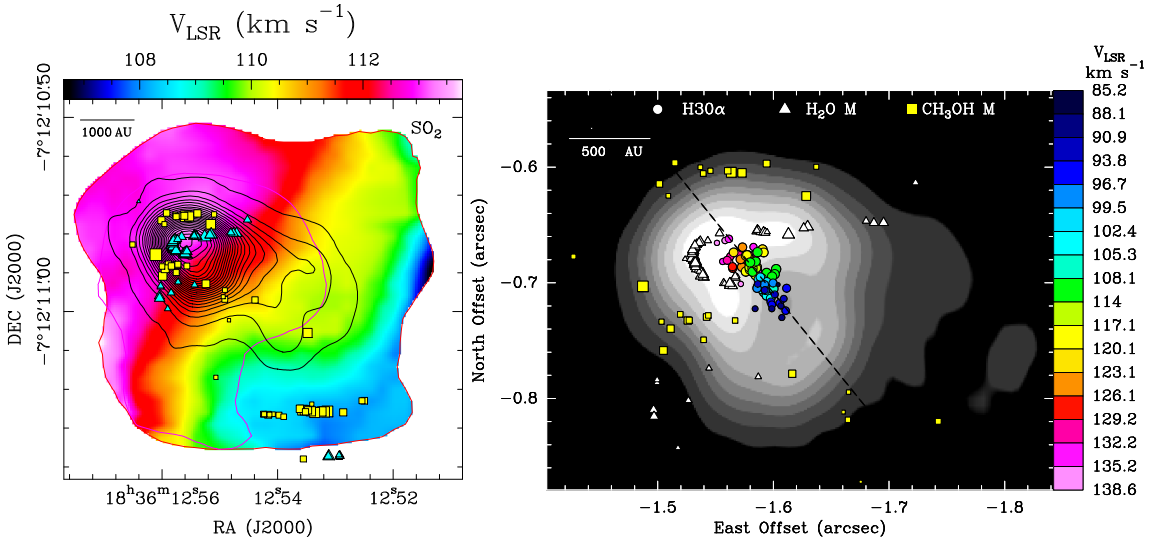

Figure 3: *Left panel:* The color map shows the intensity-averaged velocity of the SO_2 v=0 16(1,15)-15(2,14) transition in core A1. The black contours reproduce the JVLA A-Array 1.3 cm continuum. The cyan triangles and yellow squares report the VLBI positions of the 22 GHz water and 6.7 GHz methanol masers, respectively. *Right panel:* The gray-scale image represents the VLA A-Array 7 mm continuum emission observed by [1]. The white triangles and yellow squares mark the VLBI positions of the H_2O 22 GHz and CH_3OH 6.7 GHz masers, respectively. The colored dots give the channel peak positions of the H30α line emission, with colors denoting V_{LSR} as indicated in the wedge on the right of the plot. The dashed black line marks the axis of the spatial distribution of the H30α peaks.

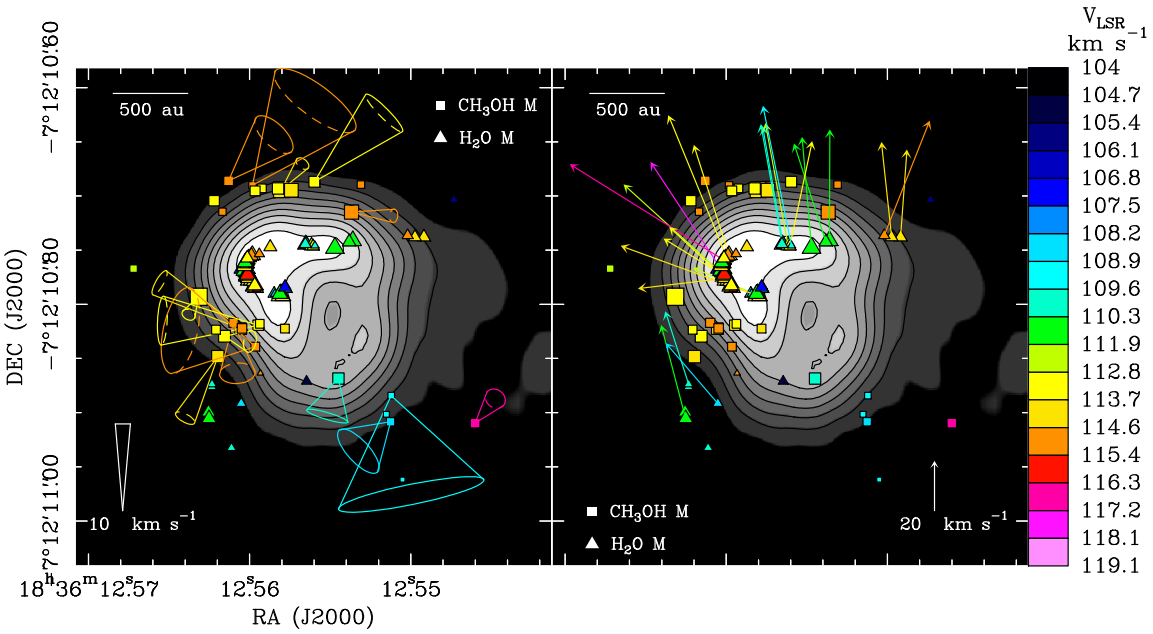

Figure 4: 3D motions of the methanol (*left panel*) and water (*right panel*) masers in G24.78+0.08 A1. In both panels, the gray-scale image and black contours reproduce the VLA A-Array 7 mm continuum observed by [1]. Colored triangles and squares report the absolute positions of the 22 GHz water and 6.7 GHz methanol masers, respectively, with colors denoting V_{LSR} as coded in the wedge on the right of the plot. In the left panel, the 3D velocities of the methanol masers are shown with cones. In the right panel, the sky-plane velocities of the water masers are indicated with arrows.

References

[1] Beltrán, M. T., R. Cesaroni, L. Moscadelli, and C. Codella (2007), "The hyperyoung H ii region in G24.78+0.08 A1." *A&A*, 471, L13–L16.

[2] Beltrán, M. T. and W. J. de Wit (2016), "Accretion disks in luminous young stellar objects." *A&ARv*, 24, 6.

[3] Bonnell, I. A., R. B. Larson, and H. Zinnecker (2007), "The Origin of the Initial Mass Function." *Protostars and Planets V*, 149–164.

[4] Moscadelli, L., R. Cesaroni, Á. Sánchez-Monge, C. Goddi, R. S. Furuya, A. Sanna, and M. Pestalozzi (2013), "A study on subarcsecond scales of the ammonia and continuum emission toward the G16.59-0.05 high-mass star-forming region." *A&A*, 558, A145.

[5] Moscadelli, L., C. Goddi, R. Cesaroni, M. T. Beltrán, and R. S. Furuya (2007), "Massive star-formation in G24.78+0.08 explored through VLBI maser observations." *A&A*, 472, 867–879.

[6] Moscadelli, L., V. M. Rivilla, R. Cesaroni, M. T. Beltrán, Á. Sánchez-Monge, P. Schilke, J. C. Mottram, A. Ahmadi, V. Allen, H. Beuther, T. Csengeri, S. Etoka, D. Galli, C. Goddi, K. G. Johnston, P. D. Klaassen, R. Kuiper, M. S. N. Kumar, L. T. Maud, T. Möller, T. Peters, F. Van der Tak, and S. Vig (2018), "The feedback of an HC HII region on its parental molecular core. The case of core A1 in the star-forming region G24.78+0.08." *A&A*, 616, A66.

[7] Moscadelli, L., Á. Sánchez-Monge, C. Goddi, J. J. Li, A. Sanna, R. Cesaroni, M. Pestalozzi, S. Molinari, and M. J. Reid (2016), "Outflow structure within 1000 au of high-mass YSOs. I. First results from a combined study of maser and radio continuum emission." *A&A*, 585, A71.

[8] Moscadelli, L. et al. (2018), "A 10 $M_{\odot}$ YSO with a Keplerian disk and a non-thermal radio jet." submitted to *A&A*.